Modeling of Cd Uptake and Efflux Kinetics in Metal-Resistant Bacterium Cupriavidus metallidurans

Hajdu, Rita; Pinheiro, Jose Paulo; Galceran, Josep; Slaveykova, Vera

Modeling of Cd Uptake and Efflux Kinetics in Metal-Resistant Bacterium *Cupriavidus metallidurans*

RITA HAJDU,[†] JOSÉ PAULO PINHEIRO,[‡,⊥] JOSEP GALCERAN,[§] AND VERA I. SLAVEYKOVA*[,†]

Environmental Biophysical Chemistry, GR-SLV-IIE-ENAC, Ecole Polytechnique Fédérale de Lausanne (EPFL), Station 2, CH-1015 Lausanne, Switzerland, IBB/CBME, Department of Physical Chemistry and Colloid Science, Wageningen University and Research Centre, Dreijenplein 6, 6703 HB Wageningen, The Netherlands, and Department of Chemistry, University of Lleida, Avda Rovira Roure 191, 25198 Lleida, Spain

Received March 3, 2010. Revised manuscript received May 2, 2010. Accepted May 7, 2010.

The Model of Uptake with Instantaneous Adsorption and Efflux, MUIAE, describing and predicting the overall Cd uptake by the metal-resistant bacterium *Cupriavidus metallidurans* CH34, is presented. MUIAE takes into account different processes at the bacteria−medium interface with specific emphasis on the uptake and efflux kinetics and the decrease in bulk metal concentration. A single set of eight parameters provides a reasonable description of experimentally determined adsorbed and internalized Cd, as well as the evolution of dissolved Cd concentrations with time, for an initial Cd concentration between 10^{-8} and 10^{-4} M, covering the situation of contaminated environments and heavily polluted effluents. The same set of parameters allowed successful prediction of the internalized and adsorbed Cd as a function of the measured free Cd ion concentration in the presence of natural and anthropogenic ligands. The findings of the present study reveal the key role of Cd efflux and bulk depletion on the overall Cd uptake by *C. metallidurans*, and the need to account for these processes to understand and improve the efficiency of the metal removal from the contaminated environment.

1. Introduction

Bioremediation and removal of toxic metals by living cells is an attractive solution for the treatment of metal-contaminated environment and industrial effluents (*1*−*3*). The ability of living cells for self-replenishment, continuous metabolic uptake of metals following adsorption, and the potential for optimization through the development of resistant species and cell surface modification offer advantages over the use of dead biomass (*2, 3*). Metal-resistant bacteria and their consortia are largely used for the decontamination of industrial effluents, as well as metal-polluted soils and mining tailings (*2*−*5*). The key processes controlling the overall metal uptake by growing cells, and, thus, their capacity to remove metals, involve transport of a metal to the organism surface, adsorption on the biological surface, and internalization (*3, 6*−*8*). It is often assumed that the adsorption process is rapid and reversible, while the internalization is slower and metabolism-dependent (*3, 6*−*8*). Once inside the cell, the metal may undergo different transformations leading to storage, detoxification, and/or efflux that can regulate the internalized content and determine metal resistance (*9, 10*). Dynamic models taking into account the key physicochemical processes, such as diffusion, adsorption, and internalization, have been successfully used to describe metal uptake in several organisms (e.g., algae, bacteria, intestinal *Caco2* cells) (*8, 11, 12*) and explored in the ecotoxicology context. However, in most bioremediation studies, the overall uptake process is described by simplified equilibrium isotherms, such as Langmuir and Freundlich, assuming that equilibrium is established between the medium and bacterial biomass (*3, 13*). The metal uptake capacity and affinity parameters of the biosorbent are obtained by fitting the experimental data obtained for a given contact time over a range of metal concentrations, but without providing information about the underlying mechanisms. Kinetics of metal sorption and uptake is modeled most often by simple (pseudo-) first and second order kinetic formalism (*13*−*15*). Different mass transfer models for metal biosorption in batch system or reactors were also reported in the literature (*16*−*18*). Furthermore, most studies considering the metal uptake by living bacteria do not distinguish between the adsorbed and internalized metal, despite their different role in removal and further recovery of the metals.

The aim of the present study is to develop a dynamic model able to describe and predict metal uptake by bacterium, considering the different processes at the bacteria−medium interface with specific emphasis on the uptake and efflux kinetics and considering the decrease in bulk metal concentration. This work extends further the research efforts to develop and refine mechanistic models able to describe and predict the dynamics of metal uptake (*8, 12, 19*−*21*), incorporating metal efflux from the cell. To the best of our knowledge, this is the first model that provides analytical expressions explicitly and simultaneously contemplating changes of the metal concentration in the medium, uptake, and efflux for living bacteria. For simplicity the model is called Model of Uptake with Instantaneous Adsorption and Efflux (MUIAE). MUIAE is developed for Cd(II), which is considered a priority pollutant (e.g., by the U.S. Environmental Protection Agency and the European Environmental Agency) and metal-resistant bacterium *Cupriavidus metallidurans* widely used in metal removal (*5*).

2. Mathematical Formulation of MUIAE

2.1. Model Starting Assumptions. Let M be a chemical specie which diffuses toward the surface of the microorganism; $c_M^*(t)$ representing its bulk concentration, which evolves with time because it is being depleted from the medium by the bacteria. M is adsorbed onto two types of adsorption sites, labeled *1*, leading to metal internalization, and *2* (not leading to metal internalization, Figure S1, insert). Each adsorption process

* Corresponding author tel: ++41 21 693 63 31; fax: ++ 41 21 693 80 70; e-mail: vera.slaveykova@epfl.ch.
[†] Ecole Polytechnique Fédérale de Lausanne (EPFL).
[‡] Wageningen University and Research Centre.
[§] University of Lleida.
[⊥] On sabbatical leave from Department of Chemistry and Biochemistry, University of the Algarve, Gambelas Campus, 8005-139 Faro, Portugal.

10.1021/es100687h
Published on Web 05/21/2010

is assumed to be fast enough, when compared with diffusion or the internalization processes, for equilibrium relationships to apply.

For type-*2* sites, the Langmuir isotherm that relates the coverage of this kind of sites ($\Gamma_2(t)/\Gamma_{max,2}$) with the concentration of M at the organism surface $c_M^0(t)$ reads:

$$\frac{\Gamma_2(t)}{\Gamma_{max,2}} = \frac{c_M^0(t)}{K_{M,2} + c_M^0(t)} \quad (1)$$

where Γ_2 stands for the surface concentration and $1/K_{M,2}$ acts as an adsorption constant (See Supporting Information (SI) for a list of symbols). Typically, a Langmuir isotherm can be linearized when $c_M^0(t)$ is negligible in front of $K_{M,2}$. The desired linearization can alternatively be obtained with better precision, by considering that the denominator in eq 1 is roughly constant because the changes in $c_M^0(t)$ are in the same order of magnitude as the bulk $c_M^*(t)$ along one experiment. For each experimental condition (i.e., [Cd(II)] $= 10^{-8}$ M, labeled as condition **I**, 10^{-6} M, labeled as condition **II** and 10^{-4} M, labeled as condition **III**), Γ_2(t) in eq 1 is approximated as:

$$\Gamma_2(t) = \Gamma_{max,2}\frac{c_M^0(t)}{K_{M,2(t)}} \approx K_{H,2}^j c_M^0(t) \quad \text{with } K_{H,2}^j = \frac{\Gamma_{max,2}}{K_{M,2} + c_{M,nominal,j}^*} \quad j = \text{I, II, or III} \quad (2)$$

so that, for instance, $K_{H,2}^I$ represents the effective adsorption constant for sites of type-*2* for a nominal bulk concentration (e.g., the concentration intended in the preparation or some other known value estimating or averaging the bulk concentration) in condition **I**.

Analogous considerations will be applied of type-*1* sites, where we distinguish—for reasons apparent in Section 3.4—two kinds of internalization sites (**a** and **b**):

$$\Gamma_1(t) = \Gamma_{max,1a}\frac{c_M^0(t)}{K_{M,1a} + c_M^0(t)} + \Gamma_{max,1,b}\frac{c_M^0(t)}{K_{M,1b} + c_M^0(t)} \approx K_{H,1}^j c_M^0(t)$$
$$\text{with} \quad K_{H,1}^j = \frac{\Gamma_{max,1a}}{K_{M,1a} + c_{M,nominal,j}^*} + \frac{\Gamma_{max,1b}}{K_{M,1b} + c_{M,nominal,j}^*} \quad j = \text{I, II, or III} \quad (3)$$

We also assume that M is taken up following a first-order kinetic process from the adsorbed amount in sites of type *1* (*7, 22*) with internalization rate constant, k_{int} yielding the uptake flux:

$$J_u(t) = k_{int}\Gamma_1(t) \quad (4)$$

The efflux J_{eff} is understood as a pumping of M from the internalized compartment out to the adsorbed sites and bulk solution, and can be thought as just the opposite of J_u. It is postulated that the efflux is proportional to what has been accumulated as internalized metal (*8, 9, 23, 24*):

$$J_{eff}(t) = k_{eff}\Phi_u(t) \quad (5)$$

where Φ_u is the internalized metal amount (in moles per unit area of cell, see SI) and k_{eff} is a constant for the efflux kinetics.

The internalized amount Φ_u changes due to the supply of the internalization flux and to the losses due to the efflux. Using eqs 3−5 and assuming that the concentration at the bacterial surface is quite similar to that in the bulk concentration, which evolve with time due to decrease in a bulk metal concentration (*12*), we reach:

$$\frac{d\Phi_u(t)}{dt} = J_u(t) - J_{eff}(t) = k_{int}K_{H,1}c_M^*(t) - k_{eff}\Phi_u(t) \quad (6)$$

To take into account the finite volume of the medium, we use the mass balance of the metal (M) over the different compartments (bulk, cell volume, and interface sites):

$$Vc_{T,M} = Vc_M^*(t) + A\Phi_u(t) + A\Gamma_1(t) + A\Gamma_2(t) \quad (7)$$

where V is the total volume of the solution and A is the total area of the cells present in this volume.

Integration of eq 6 leads to an exponential decay expression for the bulk concentration (see SI-7), from which all other quantities can be computed. For a rough estimation, in Section 4.1, we will further assume a negligible efflux (in the 20 min experiment) and a constant uptake flux (steady-state approximation):

$$\Phi_u(t) = \Phi_u(0) + \int_0^t J_u(\tau)d\tau - \int_0^t J_{eff}(\tau)d\tau \approx k_{int}\Gamma_1(t) \times t \quad (8)$$

3. Materials and Methods

3.1. Bacterial Growth Conditions. *C. metallidurans* CH34 (also known as *Ralstonia metallidurans, Alcaligenes eutrophus*) is a gram-negative soil bacterium, able to grow in the presence of millimolar concentrations of metals (*25*). *C. metallidurans* CH34 was cultured aerobically in a mineral salts liquid medium 284 (*25*) prepared in 10^{-2} M of MOPS (3-(*N*-morpholino)-propanesulfonic acid, p.a. Fluka) at pH 7.0 and complemented with 0.2% Na-gluconate as a carbon source. The cultures were agitated on a rotary shaker at 160 rpm at 30 °C. At the late log phase ($OD_{600} = 1.8 \pm 0.1$) bacteria were isolated by gentle centrifugation and washed twice with 10^{-2} M MOPS at pH 7.0.

3.2. Cd Uptake Kinetics Experiments. In the uptake kinetics study, bacteria were resuspended in 10^{-2} M of MOPS (pH 7.0) supplemented with 8×10^{-9}, 9×10^{-7}, or 9×10^{-5} M of Cd(II) as cadmium nitrate (p.a. Fluka). These concentrations were chosen as corresponding to contaminated environments and heavily polluted industrial effluents. The concentration of bacteria during each experiment was 1.36 $\pm$ 0.06 $g_{D.W.}$ L^{-1} and corresponds to a bacterial surface area of 14.12 m^2 L^{-1}. Cd uptake kinetics was followed as a function of time up to 60 min, by measuring the internalized, adsorbed, and dissolved Cd(II) concentrations in bacterial suspensions. Aliquots of 8.5 mL were taken each 5 or 10 min and bacteria were separated from the solution by gentle centrifugation at 4000 rpm. The supernatant was used to measure the dissolved metal concentration. The bacterial pellet was washed for 2 min with EDTA (ethylenediaminetetraacetic acid, ultra Fluka) 10^{-3} M at pH = 7.0 to extract Cd adsorbed to the bacterial surface (*26, 27*) which is identified with $\Gamma_2 + \Gamma_1$ (Figure S1). The amount of internalized Cd (EDTA-nonextractable, Φ_u) was determined following the digestion of the bacterial pellet with concentrated HNO_3 (Suprapur, Backer) at 100 °C during 1 h. Bulk, adsorbed, and internalized Cd concentrations were measured by inductively coupled plasma−mass spectometry (ICP-MS) (Elan DRC II, Perkin-Elmer) or by inductively coupled plasma−optical emission spectroscopy (ICP-OES) (Optima 3300 DV, Perkin-Elmer), depending on the concentration range.

3.3. Cadmium Efflux Experiments. The efflux was quantified following the decrease of the internalized Cd content over time. For this purpose, bacteria were pre-exposed to 5 $\times$ 10^{-8}, 9×10^{-7}, or 9×10^{-5} M Cd(II) for 20 min and washed with EDTA 10^{-3} M, then resuspended in MOPS 10^{-2} M. Aliquots of the bacterial suspensions (8.5 mL) were taken every 10 min over an approximately 40-min period and centrifuged. The internalized Cd content was determined

after acid digestions of the bacterial pellet and ICP-MS measurements. Bacterial density was kept the same as for uptake experiments.

3.4. Quantification of Cd Adsorption and Internalization in the Absence and Presence of Ligands. Internalized and adsorbed Cd contents in *C. metallidurans* exposed to increasing Cd(II) concentrations from 10^{-9} to 10^{-3} M were determined at constant contact time of 20 min. Since the uptake is directly related to the free rather than the total Cd(II) concentrations (*6*), the experiments were performed in the absence and presence of citric (CA), nitrilotriacetic (NTA), Elliot Soil (EHA), and Pahokee Peat (PPHA) humic acids (International Humic Substances Society, St. Paul). Stock solutions of 1 g L^{-1} were prepared in Milli-Q water, equilibrated overnight, and stored in dark at 4 °C. The concentrations of EHA and PPHA were fixed at 50 mg L^{-1}, while the total concentrations of Cd(II) varied between 10^{-7} and 10^{-5} M. Free cadmium ion concentrations, $[Cd^{2+}]$, were measured by ion exchange technique as detailed elsewhere (*27*). Internalized and adsorbed Cd concentrations used as measures of Cd uptake were expressed in mol m^{-2} taking the area of single cell to be 3.5×10^{-12} m^2 $cell^{-1}$.

4. Results

To describe the Cd uptake and efflux by living bacteria, MUIAE requires eight relevant parameters: six coupled parameters related with the equilibrium binding to the internalization and mere adsorption sites ($K_{M,1a}$, $K_{M,1b}$, $K_{M,2}$, $\Gamma_{max,1a}$, $\Gamma_{max,1b}$, $\Gamma_{max,2}$) and two kinetics parameters related with uptake (k_{int}) and efflux (k_{eff}). The iterative fitting procedure to evaluate these parameters is detailed in the next subsections and can be summarize as follows. The initial estimates of the Cd binding characteristics were obtained from the adsorption and internalization experiments. Then, the rate constants k_{int} and k_{eff} were evaluated from the independent Cd uptake kinetics experiments. The obtained single set of parameters was used next to simulate the adsorbed and internalized Cd concentrations in independent efflux and accumulation experiments in the presence of environmental ligands.

4.1. Cd Adsorption and Internalization. Evaluation of Equilibrium Parameters. For a constant contact time, the amount of the adsorbed Cd increased with Cd(II) concentration in the solution. A first estimation of the equilibrium parameters $\Gamma_{max,2}$, $K_{M,2}$ (characterizing Cd binding to mere adsorption sites) and $\Gamma_{max,1}$, $K_{M,1b}$ (Cd binding to internalization sites) was obtained from the fitting of the adsorbed Cd content versus bulk Cd(II) concentration (Figure 1A) with a two-sites Langmuir isotherm. $\Gamma_{max,2}$ of 4.96×10^{-6} mol m^{-2} and $K_{M,2}$ of 7.1×10^{-1} mol m^{-3}, $\Gamma_{max,1b}$ of 4.46×10^{-7} mol m^{-2} and $K_{M,1b}$ of 1.19×10^{-3} mol m^{-3} were estimated.

Further refinement of the adsorption characteristics was made by using Cd internalization data (Figure 1B). Internalized Cd is considered as the EDTA non-extractable fraction (Figure S1). The fit of the experimental data with eq 8 was only possible by considering two types of internalization sites: (a) high-affinity internalization sites, acting at low Cd(II) concentrations, and (b) low-affinity internalization sites that are acting at high Cd(II) concentrations. $K_{H,1a}$ and $K_{H,1b}$ were obtained from the plot of the internalized Cd amount versus bulk Cd^{2+} concentration (Figure 1B), using a value of $k_{int} = 8.3 \times 10^{-4}$ s^{-1} as a first approximation. This initial estimate lies within the range of the internalization rate constants published in the literature (i.e., 10^{-4} to 10^{-2} s^{-1} for the toxic trace metals (*7*)), as well as corresponds to $k_{int} \times t = 1$ for an exposure time t of 20 min. The high-affinity sites of $\Gamma_{max,1a}$ appear in much smaller number than the low-affinity ones and, thus, cannot be estimated from the adsorbed amount. On the other hand, their affinity, $K_{M,1a}$ is much higher. So, taking the low affinity sites estimation obtained from the adsorbed data and fitting the internalization data allows the decoupling of $K_{H,1}$ components. This yielded initial values of $\Gamma_{max,1a} = 3.98 \times 10^{-9}$ mol m^{-2} and $K_{M,1a} = 8.47 \times 10^{-6}$ mol m^{-3} for the high-affinity internalization sites and the refining of the low-affinity sites values gave $\Gamma_{max,1b} = 5.49 \times 10^{-7}$ mol m^{-2} and $K_{M,1b} = 1.08 \times 10^{-2}$ mol m^{-3}.

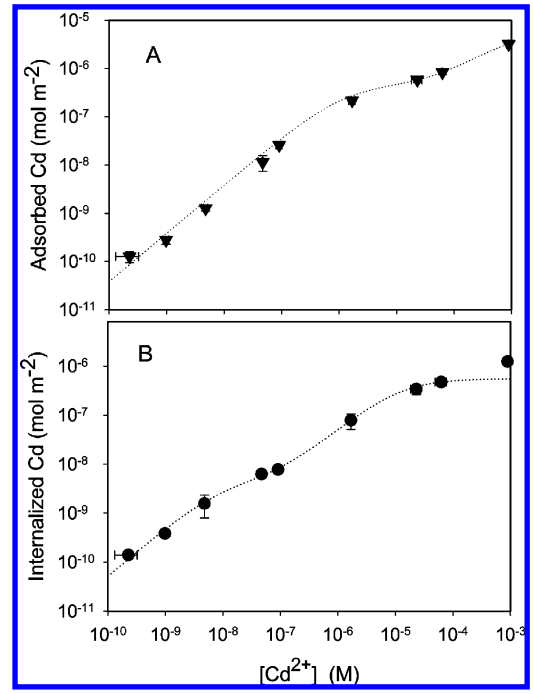

FIGURE 1. Log−log plot of adsorbed ($\Gamma_1+\Gamma_2$; A) and internalized (Φ_u: B) Cd content versus increasing bulk free Cd ion concentrations (pH 7.0 and ionic strength 5×10^{-3} M) at 20 min of exposure time. Error bars were calculated in duplicate or triplicate experiments and are represented when bigger than symbol. The lines represent the respective fits (using the full Langmuirian expressions before linearization) with eqs 1 and 2 for adsorbed Cd and eq 8 in the case of internalized Cd.

4.2. Cd Uptake and Efflux. Kinetic Parameters Determination. Apart from internalization and adsorption parameters, the model needs the rate constants of uptake, k_{int} and efflux, k_{eff}. They were fitted simultaneously from the uptake kinetics experiments (Figure 2) using the initial estimates of Γ_{max} and K_M obtained in Section 4.1. The evolution of the internalized, adsorbed, and bulk Cd(II) versus contact time at initial Cd(II) concentration of 8×10^{-9} M, was fitted to exponential-like expressions derived from eq SI-7 with a k_{int} of 7.08×10^{-4} s^{-1} and a k_{eff} of 7.00×10^{-4} s^{-1} (Figure 2A). The data fitting at this concentration was very sensitive to k_{int}, k_{eff}, and $K_{H,1a}$ and less sensitive to $K_{H,1b}$ and $K_{H,2}$. The uptake parameters were further adjusted by using the Cd uptake kinetic data at the highest initial Cd(II) concentration of 9×10^{-5} M (Figure 2C). The fit quality was quite sensitive to $K_{H,1b}$ and $K_{H,2}$ and required a fine-tuning of $\Gamma_{max,1b}$, $K_{M,1b}$, and $K_{M,2}$. Additional refinement of the uptake and efflux parameters was obtained by using the uptake kinetics results obtained at 10^{-6} M Cd(II) (Figure 2B). These optimized kinetic and equilibrium parameters (Table 1) are further validated by simulating the changes in the internalized, adsorbed, and bulk Cd(II) concentrations as a function of the time (Figure 2), as well as the independent efflux (Figure 3) and accumulation experiments (Figure 4).

4.3. Validation of the Model and Its Parameters against Cd Efflux Experiments. The efflux experiments follow the changes of the internalized Cd content over time for bacteria pre-exposed to a given Cd(II) concentration and resuspended in the Cd-free medium. A good agreement between the MUIAE simulated and experimentally determined amounts

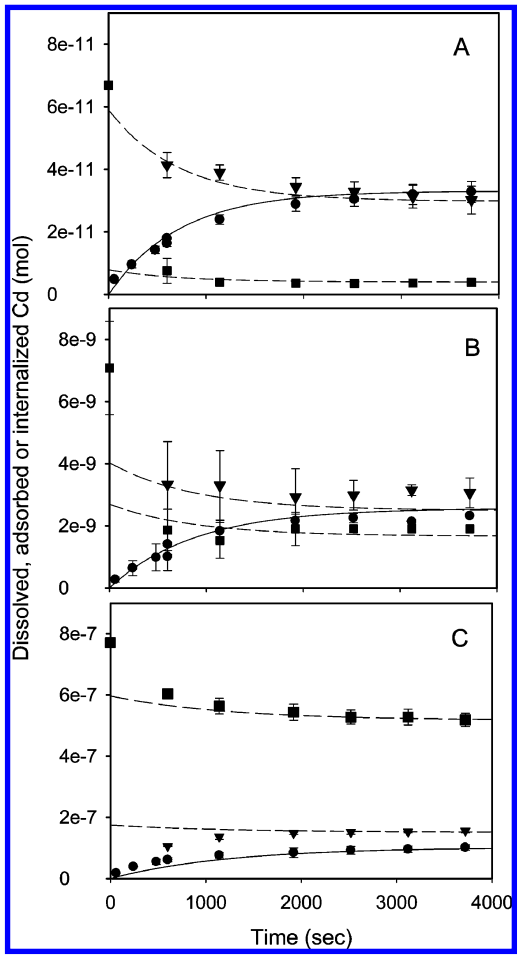

FIGURE 2. Internalized (•), adsorbed (▼), and bulk (■) Cd amounts (in moles in 8.5 mL) versus contact time in the uptake experiments: (A) 8×10^{-9} M, (B) 9×10^{-7} M, (C) 9×10^{-5} M initial Cd(II) concentration. Experimental data are presented by full symbols, the MUIAE fit by lines: internalized (—), adsorbed (— —), and bulk (- - -). Error bars were calculated in duplicate experiments and are drawn when bigger than symbol. Lines stand for the model amounts computed starting with eq SI-7 and parameters in Table 1.

of internalized Cd in the efflux experiment is obtained in the probed large concentration range, as illustrated for initial Cd(II) concentrations of 5×10^{-8}, 9×10^{-7}, and 9×10^{-5} M (Figure 3).

4.4. Cd Accumulation Experiments in the Presence of Ligands. Furthermore with the parameters in Table 1, simplified equations reproduce reasonably well the adsorbed and internalized Cd contents for various bulk free Cd ion concentrations in the presence of natural and anthropogenic ligands such as citrate, NTA, and humic acids (solid lines in Figure 4A and B).

5. Discussion

With a single set of parameters, the MUIAE describes both kinetic data of Cd internalization and efflux over a large initial Cd(II) concentration range representative of slightly to heavily polluted media. The modeling results clearly reproduce the observed evolutions of adsorbed Cd in the cell surface and bulk Cd concentration decrease (see below). The optimized values for $\Gamma_{max,2}$ and K_{M2} (Table 1) were consistent with the binding sites characteristics reported for *C. metallidurans*: site density of 0.42 mmol g^{-1} and pK_a of 3.9 for carboxylic, 0.12 mmol g^{-1} and 6.8 for phosphate, and 0.45 mmol g^{-1} and 9.4 for amine binding sites were found with a proton titration of the bacterial cell walls (*28*). At pH 7.0 only carboxylic and phosphate groups are considered as deprotonated, so the maximal density of the binding sites available for Cd should be smaller than 2.96×10^{-5} mol m^{-2}, value equivalent to the sum of the density of the carboxylic and phosphate groups. Furthermore, the initial estimate for log ($1/K_{M,2}$) of 3.15 is close to the values of Cd exchange with binding sites for the carboxylic sites (log K 3.6 for carboxylic, 4.7 for phosphate, and 5.0 for amine groups (*29*)). In addition, the two types of internalization sites (Figure 1B) were consistent with existing genomic and proteomic data reporting two major Cd transporters in *C. metallidurans*: the MIT (metal ion transport) and P-type ATPase (*30, 31*).

In the uptake kinetics experiments, when bacteria were exposed to 8×10^{-9} M Cd(II), a rapid about 14-fold decrease in dissolved Cd(II) amount was observed (Figure 2A). The adsorbed Cd attained amounts greater than those for both bulk and internalized Cd. The amount of the internalized Cd increased over time tending to a plateau at times longer than 40 min. At 9×10^{-7} M Cd(II), the amount of bulk Cd(II) decreased only 4 times and was lower than the adsorbed Cd, but comparable to the internalized Cd. Similar trends in the time evolution of the adsorbed and internalized Cd contents were obtained when bacteria were exposed to 9×10^{-5} M total Cd(II) (Figure 2C). However, dissolved Cd(II) decreased only 1.3 times and was higher than both the adsorbed and internalized fractions, as expected for such a high concentration of Cd(II) in solution. In the entire Cd(II) concentration range, the amount of internalized Cd increases rapidly in the first few minutes and, then, tends to a plateau. Even significant at low Cd(II) concentrations, the bulk depletion alone is insufficient to explain the plateau in the internalized Cd. Assuming that the equilibrium between bulk and cell surface is instantaneous and reversible, the observed decrease in adsorbed Cd can be linked to the decrease in the dissolved Cd(II) in the bacterial medium. The appearance of a plateau in the bulk concentration cannot be explained with just the bulk depletion effect. Indeed, taking $k_{eff} = 0$ results in a nil bulk concentration for the limit of time infinitely long (against the experimental observation of a plateau in the internalized amount). Since bulk Cd concentration decrease is important, the average values of $c_M^*(t)$ were used in the model as "nominal" values of bulk concentrations in eqs 2 and 3.

The modeling of Cd uptake by bacteria in a wide concentration range helps in the understanding of the role of the key processes involved and their interconnection. For example, at high Cd(II) concentrations (e.g., 10^{-4} M) the fit quality was quite sensitive to $K_{H,1b}$ and $K_{H,2}$, demonstrating the importance of Cd binding to the low-affinity internalization and adsorption sites for the overall uptake. By contrast, the data fitting at low Cd(II) concentration was very sensitive to rate constants k_{int} and k_{eff} as well as to the $K_{H,1a}$ (high-affinity internalization sites) and less sensitive to $K_{H,1b}$ and $K_{H,2}$, characterizing the low-affinity internalization and mere adsorption sites. Furthermore, neglecting Cd efflux resulted in a significant underestimation of the adsorbed and overestimation of the internalized Cd content, even at low Cd(II) concentrations. These findings are in line with the literature demonstrating that the metal efflux is one of the most important metal resistant mechanisms for this bacterium. Indeed, the existence of several efflux systems including CDF (cation diffusion facilitators), RND (resistance nodulation division) efflux family, and P-type ATPases which are energy-dependent in *C. metallidurans* CH34 (*9, 30, 32*). The Cd efflux rate constant $k_{eff} = 7.00 \times 10^{-4}$ s^{-1} of this metal-resistant bacterium is estimated to be 78 times higher than that of the metal-sensitive bacterium *Bacillus firmus*, where k_{eff} for Cd is around 9×10^{-6} s^{-1} (*26, 33*). The Cd efflux rate constant for the cynobacterium *Microcystis aeruginosa* was found to be between 8×10^{-6} and 1.5×10^{-5} s^{-1} (*34*) which is approximately 88 to 46 times smaller than k_{eff} found for

TABLE 1. Summary of the Fitted Parameters Characterizing Cd Uptake and Efflux Kinetics of Cd(II) by Bacterium *C. metallidurans*, pH 7.0, Ionic Strength 5×10^{-3} M

$\Gamma_{max,1a}$ (mol m^{-2})	$K_{M,1a}$ (mol m^{-3})	$\Gamma_{max,1b}$ (mol m^{-3})	$K_{M,1b}$ (mol m^{-3})	$\Gamma_{max,2}$ (mol m^{-2})	$K_{M,2}$ (mol m^{-3})	k_{int} (s^{-1})	k_{eff} (s^{-1})
3.98×10^{-9}	8.47×10^{-6}	9.88×10^{-7}	1.40×10^{-2}	4.96×10^{-6}	5.30×10^{-1}	7.91×10^{-4}	7.00×10^{-4}

C. metallidurans. This difference is probably due to the fact that the resistant microorganisms possess more efficient efflux systems than nonresistant bacteria (*10*).

In spite of reproducing the major features experimentally observed, MUIAE does not satisfactorily predict the adsorbed and dissolved Cd(II) concentrations in the first few minutes of the exposure (Figure 2). The discrepancy between the predicted and experimentally determined values increases for lower initial Cd(II) concentrations, being largest for the bacterial suspensions supplemented with 8×10^{-9} M Cd(II). Thus, further improvements of the model predictions could perhaps require a more explicit consideration of the transient diffusion fluxes (*19, 35*). However, an estimation of the time needed to reach 10% proximity to the steady-state flux (more details in the SI) yielded 1.2 s. This suggests that the role of the transient diffusion fluxes could be of minor importance and other physical, chemical, or biological factors should be taken into consideration. Nevertheless, MUIAE allows for the discrimination between equilibrium and kinetic parameters for bacteria at measuring times longer than ca. 10 min, generally applied for the metal removal.

Overall, MIUAE is a first dynamic model integrating different phenomena at the bacteria−medium interface including the metal efflux, which is considered as the major mechanism determining metal resistance of bacteria such as *C. metallidurans*. This work has used varied experiments to focus on specific steps of the complex interactions of metal and bacteria, such as Cd accumulation, uptake, and efflux kinetics experiments. The concentration range covered low (i.e., when metal depletion is important) and high (i.e., when metal reduction is less significant) metal concentrations, thus allowing a detailed exploration at overall biouptake process dynamics. The combination of the theoretical and experimental approach of the present study demonstrated the peculiar interplay between adsorption, internalization, and efflux as well as metal depletion, these phenomena all affecting the amount of the metal accumulated in bacteria. Understanding and quantifying the processes controlling the metal−bacterial interactions is a prerequisite for the correct interpretation and prediction of the metal uptake and efficiency of the toxic metal removal from contaminated environment. According to the obtained results, the reduction of the metal in the medium and the efflux from the cell may

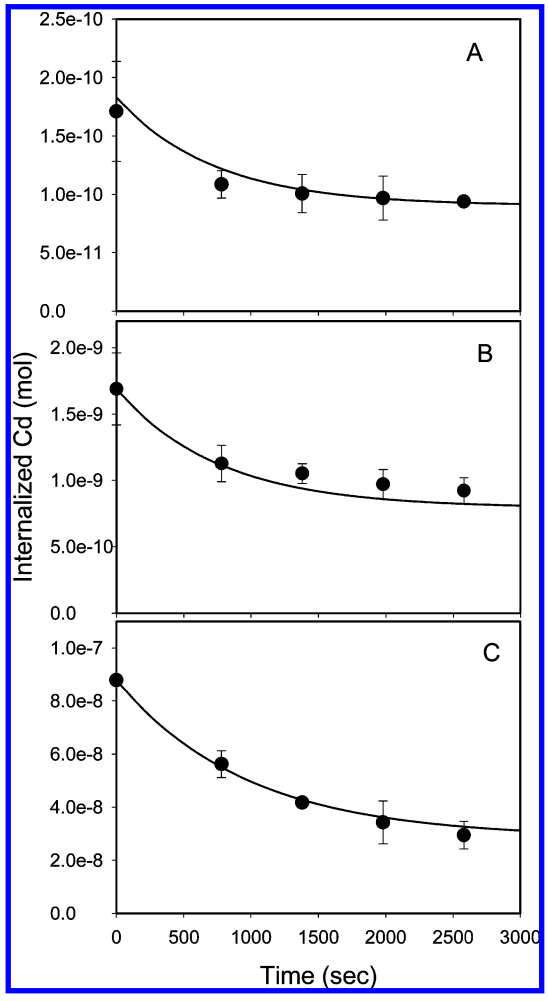

FIGURE 3. Comparison between the calculated (lines) and experimentally determined (points) internalized Cd ($A\Phi_u$ moles in 8.5 mL) versus time in the efflux experiments. Bacteria were pre-exposed at initial Cd(II) concentrations of (A) 5×10^{-8} M Cd(II), (B) 9×10^{-7} M Cd(II), and (C) 9×10^{-5} M Cd(II). Error bars were calculated in duplicate experiments and are presented when bigger than symbol. MUIAE calculations performed with eq SI-7 and parameters in Table 1.

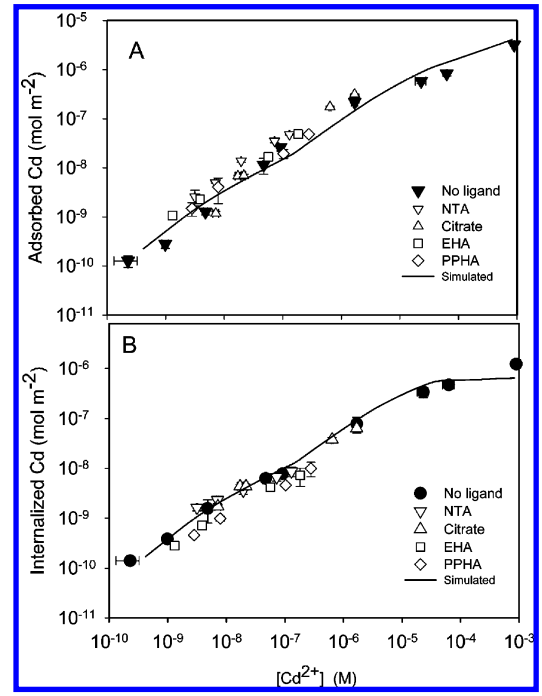

FIGURE 4. Log−log plot of adsorbed ($\Gamma_1+\Gamma_2$; A) and internalized (Φ_u; B) Cd content versus increasing measured bulk free Cd^{2+} concentrations, in the absence of ligands (•) and in the presence of NTA (▽), citrate (▼), EHA (*), and PPHA (◇) (pH 7.0 and ionic strength 5×10^{-3} M). Error bars were calculated in duplicate or triplicate experiments and are represented when bigger than symbol. Solid lines stand for the numerical calculations using eqs 1 and 2 for adsorbed Cd and eq 8 for internalized Cd. Parameters from Table 1.

limit both the adsorption and the internalization, and thus the overall metal uptake.

Acknowledgments

Funding for this work by the Swiss National Science Foundation (PP002 102640 and PP022 118989) is warmly acknowledged by V.I.S. and R.H. J.G. acknowledges financial support form the Spanish Ministry of Science and Innovation (Projects CTQ2006-14385 and CTQ2009-07831) and from the "Comissionat per a Universitats i Recerca del Departament d'Innovació, Universitats i Empresa de la Generalitat de Catalunya". J.P.P. acknowledges funding received by "IBB/CBME, LA, FEDER/POCI 2010" and a sabbatical grant SFRH/BSAB/855/2008 from Fundação para a Ciência e Tecnologia, Portugal.

Supporting Information Available

Details about the MUIAE development, list of the symbols, and simplified schema of known Cd uptake and efflux systems by gram-negative bacterium *C. metallidurans* CH34, estimation of the transient regime for diffusion. This information is available free of charge via the Internet at http://pubs.acs.org.

Literature Cited

(1) Tabak, H.; Lens, P.; Van Hullebusch, E.; Dejonghe, W. Developments in bioremediation of soils and sediments polluted with metals and radionuclides−1. Microbial processes and mechanisms affecting bioremediation of metal contamination and influencing metal toxicity and transport. *Rev. Environ. Sci. Biotechnol.* **2005**, *4*, 115–156.

(2) Malik, A. Metal bioremediation through growing cells. *Environ. Int.* **2004**, *30*, 261–278.

(3) Gadd, G. M. Biosorption: Critical review of scientific rationale, environmental importance and significance for pollution treatment. *J. Chem. Technol. Biotechnol.* **2009**, *84*, 13–28.

(4) Diels, L.; Spaans, P.; Van Roy, S.; Hooyberghs, L.; Ryngaert, A.; Wouters, H.; Walter, E.; Winters, J.; Macaskie, L.; Finlay, J.; Pernfuss, B.; Woebking, H.; Pumpel, T.; Tsezos, M. Heavy metals removal by sand filters inoculated with metal sorbing and precipitating bacteria. *Hydrometallurgy* **2003**, *71*, 235–241.

(5) Nies, D. H. Heavy metal-resistant bacteria as extremophiles: Molecular physiology and biotechnological use of *Ralstonia sp.* CH34. *Extremophiles* **2000**, *4*, 77–82.

(6) Campbell, P. G. C. Interactions between trace metals and aquatic organisms: A critique of the free-ion activity model. In *Metal Speciation and Bioavailability in Aquatic Systems*; Tessier, A. A., Turner, D. R., Eds.; J. Wiley and Sons: Chichester, 1995; pp 45−102.

(7) Wilkinson, K. J.; Buffle, J. Critical evaluation of physicochemical parameters and processes for modelling the biological uptake of trace metals in environmental (aquatic) systems. In *Physicochemical Kinetics and Transport at Biointerfaces*; Van Leeuwen, H. P., Koester, W., Eds.; J. Wiley and Sons: Chichester, 2004; pp 447−533.

(8) Galceran, J.; Van Leeuwen, H. P. Dynamics of biouptake processes: The role of transport, adsorption and internalisation. In *Physicochemical Kinetics and Transport at Biointerfaces*; Van Leeuwen, H. P., Koester, W., Eds.; J Wiley and Sons: Chichester, 2004; pp 147−203.

(9) Nies, D. H. Efflux-mediated heavy metal resistance in prokaryotes. *FEMS Microbiol. Rev.* **2003**, *27*, 313–339.

(10) Bruins, M. R.; Kapil, S.; Oehme, F. W. Microbial resistance to metals in the environment. *Ecotox. Environ. Safe.* **2000**, *45*, 198–207.

(11) Van Leeuwen, H. P. Metal speciation dynamics and bioavailability: Inert and labile complexes. *Environ. Sci. Technol.* **1999**, *33*, 3743–3748.

(12) Pinheiro, J. P.; Galceran, J.; Van Leeuwen, H. P. Metal speciation dynamics and bioavailability: Bulk depletion effects. *Environ. Sci. Technol.* **2004**, *38*, 2397–2405.

(13) Febrianto, J.; Kosasih, A. N.; Sunarso, J.; Ju, Y.-H.; Indraswati, N.; Ismadji, S. Equilibrium and kinetic studies in adsorption of heavy metals using biosorbent: A summary of recent studies. *J Haz. Mater.* **2009**, *162*, 616–645.

(14) Bai, H.-J.; Zhang, Z.-M.; Yang, G.-E.; Li, B.-Z. Bioremediation of cadmium by growing *Rhodobacter sphaeroides*: Kinetic characteristic and mechanism studies. *Biores. Technol.* **2008**, *99*, 7716–7722.

(15) Veglio, F.; Beolchini, F. Removal of metals by biosorption: A review. *Hydrometallurgy* **1997**, *44*, 301–316.

(16) Yang, J.; Volesky, B. Cadmium biosorption rate in protonated *Sargassum* biomass. *Environ. Sci. Technol.* **1999**, *33*, 751–757.

(17) Choy, K. K. H.; Mckay, G. Sorption of cadmium, copper, and zinc ions onto bone char using crank diffusion model. *Chemosphere* **2005**, *60*, 1141–1150.

(18) Vilar, V. J. P.; Botelho, C. M. S.; Boaventura, R. A. R. Kinetics modelling of biosorption by algal biomass from binary metal solutions using batch contactors. *Biochem. Eng. J.* **2008**, *38*, 319–325.

(19) Galceran, J.; Monné, J.; Puy, J.; Van Leeuwen, H. P. Transient biouptake flux and accumulation by microorganisms: The case of two types of sites with Langmuir adsorption. *Mar. Chem.* **2006**, *99*, 162–176.

(20) Van Leeuwen, H. P.; Town, R. M.; Buffle, J.; Cleven, R. F. M. J.; Davison, W.; Puy, J.; Van Riemsdijk, W. H.; Sigg, L. Dynamic speciation analysis and bioavailability of metals in aquatic systems. *Environ. Sci. Technol.* **2005**, *39*, 8545–8556.

(21) Van Leeuwen, H. P.; Pinheiro, J. P. Speciation dynamics and bioavailability of metals. Exploration of the case of two uptake routes. *Pure Appl. Chem.* **2001**, *73*, 39–44.

(22) Slaveykova, V. I.; Wilkinson, K. J. Physicochemical aspects of lead bioaccumulation by *Chlorella vulgaris*. *Environ. Sci. Technol.* **2002**, *36*, 969–975.

(23) Mirimanoff, N.; Wilkinson, K. J. Regulation of Zn accumulation by a freshwater gram-positive bacterium (*Rhodococcus opacus*). *Environ. Sci. Technol.* **2000**, *34*, 616–622.

(24) Nies, D. H. The cobalt, zinc, and cadmium efflux system CZCABC from *Alcaligenes eutrophus* functions as a cation-proton antiporter in *Escherichia coli*. *J. Bacteriol.* **1995**, *177*, 2707–2712.

(25) Mergeay, M.; Nies, D. H.; Schlegel, H. G. M.; Gerits, J.; Charles, P.; Van Gijsegem, F. *Alcaligenes eutrophus* CH34 is a facultative chemolithotroph with plasmid-bound resistance to heavy metals. *J. Bacteriol.* **1985**, *162*, 328–334.

(26) Keung, C. F.; Guo, F.; Qian, P.; Wang, W. X. Influences of metal-ligand complexes on the cadmium and zinc biokinetics in the marine bacterium *Bacillus firmus*. *Environ. Toxicol. Chem.* **2008**, *27*, 131–137.

(27) Slaveykova, V. I.; Dedieu, K.; Parthasarathy, N.; Hajdu, R. Effect of competing ions and complexing organic substances on the cadmium uptake by the soil bacterium *Sinorhizobium meliloti*. *Environ. Toxicol. Chem.* **2009**, *28*, 741–748.

(28) Guine, V.; Martins, J. M. F.; Causse, B.; Durand, A.; Gaudet, J. P.; Spadini, L. Effect of cultivation and experimental conditions on the surface reactivity of the metal-resistant bacterium *Cupriavidus metallidurans* CH34 to protons, cadmium and zinc. *Chem. Geol.* **2007**, *236*, 266–280.

(29) Guine, V.; Spadini, L.; Sarret, G.; Muris, M.; Delolme, C.; Gaudet, J. P.; Martins, J. M. F. Zinc sorption to three gram-negative bacteria: Combined titration, modeling, and EXAFS study. *Environ. Sci. Technol.* **2006**, *40*, 1806–1813.

(30) Von Rozycki, T.; Nies, D. H.; Saier, M. H. Genomic analyses of transport proteins in *Ralstonia metallidurans*. *Comp. Func. Genomics* **2005**, *6*, 17–56.

(31) Nies, D. Microbial heavy-metal resistance. *Appl. Microbiol. Biotechnol.* **1999**, *51*, 730–750.

(32) Mergeay, M.; Monchy, S.; Vallaeys, T.; Benotmane, A.; Bertin, P.; Taghavi, S.; Van Der Lelie, D.; Auquier, V.; Dunn, J.; Wattiez, R. *Ralstonia metallidurans*, a bacterium specifically adapted to toxic metals: Towards a catalogue of metal-responsive genes. *FEMS Microbiol. Rev.* **2003**, *27*, 385–410.

(33) Chen, D.; Qian, P. Y.; Wang, W. X. Biokinetics of cadmium and zinc in a marine bacterium: Influences of metal interaction and pre-exposure. *Environ. Toxicol. Chem.* **2008**, *27*, 1794–1801.

(34) Zeng, J.; Yang, L.; Wang, W.-X. Acclimation to and recovery from cadmium and zinc exposure by a freshwater cyanobacterium *Microcystis aeruginosa*. *Aquat. Toxicol.* **2009**, *93*, 1–10.

(35) Galceran, J.; Monne, J.; Puy, J.; Van Leeuwen, H. P. The impact of the transient uptake flux on bioaccumulation: Linear adsorption and first-order internalization coupled with spherical semi-infinite mass transport. *Mar. Chem.* **2004**, *85*, 89–102.

ES100687H